

Block Nearest Neighbor Gaussian processes for large datasets

Zaida C. Quiroz¹, Marcos O. Prates², and Dipak K. Dey³

¹Pontificia Universidad Catlica del Perú

²Universidade Federal de Minas Gerais

³University of Connecticut

December 21, 2024

Abstract

This work develops a valid spatial block-Nearest Neighbor Gaussian process (block-NNGP) for estimation and prediction of location-referenced large spatial datasets. The key idea behind our approach is to subdivide the spatial domain into several blocks which are dependent under some constraints. The cross-blocks capture the large-scale spatial variation, while each block capture the small-scale dependence. The block-NNGP is embedded as a sparsity-inducing prior within a hierarchical modeling framework. Markov chain Monte Carlo (MCMC) algorithms are executed without storing or decomposing large matrices, while the sparse block precision matrix is efficiently computed through parallel computing. We also consider alternate MCMC algorithms through composite sampling for faster computing time, and more reproducible Bayesian inference. The performance of the block-NNGP is illustrated using simulation studies and applications with massive real data, for locations in the order of 10^4 .

KEY WORDS: Bayesian hierarchical models, block-NNGP, geostatistics, large datasets, kd-tree, MCMC, parallel computing.

1 Introduction

New technologies such as GPS and remote sensing enable the collection of massive amounts of high-resolution geographically referenced observations over large areas. When nearby georeferenced units are associated in some way, these data are quite often analyzed through spatial random fields, which are usually based on Gaussian fields (GF). It is well-known that computations over GF can be prohibitive when the number of locations is large, since many calculations depend on its dense covariance and precision matrix.

A useful approach to deal with large spatial datasets proceeds inducing sparsity in the precision matrix through Gaussian Markov random fields (GMRF), assuming that the spatial correlation between pairs of distantly located observations is nearly zero (Rue and Tjelmeland, 2002). In particular, this sparsity can be achieved either through stochastic partial differential equations (SPDE - Lindgren et al. 2011) or the Nearest Neighbor Gaussian process (NNGP- Datta et al. 2016). In the SPDE approach, a GF with a Matérn covariance function is the solution of a specific SPDE (Whittle, 1954), so it can be approximated to a GMRF through finite element methods Lindgren et al. 2011). On the other hand, the NNGP is a well-defined spatial GMRF, built from lower-dimensional conditional distributions, based on the nearest neighbor observations of each observation.

The main advantage of NNGP over the SPDE approach, is that it works for any valid covariance function. Nevertheless, one drawback of the NNGP is that it needs to pre-determine a collection of the “past” neighbors, but in spatial settings, the locations are not naturally ordered. Guinness (2018) proves that random orderings can give dramatically sharper approximations than default coordinate-based orderings. However, the information of “non-past” nearest neighbors is not considered and some small-scale spatial dependence may be lost.

Another approach to deal with computationally intractable large matrices of GF is the spatial blocking, that is, the partition of the spatial domain into blocks. This approach was often restricted to covariance matrices, ignoring the dependence between different blocks. Stein (2013) and Bolin and Wallin (2016) showed that this simple approach is better than covariance tapering approaches, methods that set “distant” observations of the covariance matrix into zero to get its sparsity. Kim et al. (2005) presented a similar approach but their method automatically decomposes the spatial domain into disjoint blocks.

Following the blocking strategies, Stein et al. (2004) used independent blocks of observations to build a composite-likelihood function. While Caragea and Smith (2007) and Eidsvik et al. (2014) allowed some dependence between blocks. They built composite-likelihood functions through conditionally independent blocks of observations. Moreover, Eidsvik et al. (2014) proposed a unified framework for both parameter estimation and prediction, but it is too restrictive, since it only fit Gaussian response variables through frequentist inference.

This paper merges the NNGP and blocking approaches proposed by Datta et al. (2016) and Eidsvik et al. (2014). First, we assume that pairs of blocks are conditionally independent given some blocks, and then we extend the NNGP theory to get a new valid GMRF called block-NNGP. This GMRF enables a consistent way to combine parameter estimation and spatial prediction. The first goal of the block-NNGP is to capture the spatial dependence at all scales, because the cross-blocks are able to capture the large-scale spatial dependence while the small-scale spatial dependence is captured through the observations inside each

block. The second contribution of this paper is that we are able to perform parallel inference for massive distributed spatial data. It is scalable to massive datasets, it only need to store “small” dense matrices to compute the precision matrix of the block-NNGP through faster parallel computation reducing computational burden, without ignoring spatial dependence between the data.

Finally, to perform inference we adopt a Bayesian framework to demonstrate the full inferential capabilities in terms of estimation, prediction and goodness of fit, of the block-NNGP hierarchical models and parameters therein. In particular, the parameters were estimated through the collapsed MCMC method (Finley et al., 2017) to improve convergence and run time. This algorithm enjoys the frugality of a low-dimensional MCMC chain but allows for full recovery of the latent random effects.

The paper is organized as follows. Section 2 gives the details of the proposed block-NNGP process. In Section 4, simulations are assessed for the predictive performance of the proposed process. An example with real data in Section 5 illustrates the benefits of the proposed process when the data size is large. Some discussions are given in Section 6.

2 Block NNGP process

Assume that $w(s) \sim \text{GP}(0, C(\theta))$ defined for all $s \in D \subset \mathbb{R}^2$, where $C(\theta)$ is any valid covariance function. Let $S = \{s_1, \dots, s_n\}$ be a fixed set of locations in D . Then the joint density of $w_S = (w(s_1), \dots, w(s_n))'$ can be written as

$$p(w_S) = p(w(s_1)) \prod_{i=2}^n p(w(s_i) | w(s_1), \dots, w(s_{i-1})). \quad (1)$$

Vecchia (1988) proposed to replace the conditioning sets on the right-hand side of Equation (1) with conditioning sets of size at most m , where $m \ll n$. In particular, Datta et al. (2016) propose to use some fixed number of nearest neighbors observations from the “past”, then Equation (1) is approximated by $\tilde{p}(w_S) = p(w(s_1)) \prod_{i=2}^n p(w(s_i) | w(s_{i_m}))$, where $w(s_{i_m})$ are the neighboring observations of $w(s_i)$. This approach seems very reasonable, since correlations between pairs of distant locations are nearly zero, and little information might be lost when taking them to be conditionally independent given intermediate locations. They also proved that $\tilde{p}(w_S)$ is a valid joint distribution for w_S , which is used to built up a valid spatial process called NNGP, thus the traditional GP is replaced by the NNGP.

Stein et al. (2004) proposed a generalization of the Vecchia approximation, a restricted version of the conditional probability approximation, where the joint density of Equation (1) is approximated by assuming a partition of w_S in vectors of non uniform lengths and some conditioning vector sets of each vector. Here we extend the NNGP introducing another valid spatial process through such approximation built on blocks of data. In particular, we consider a partition of the region D into M blocks b_1, \dots, b_M , with $\bigcup_{k=1}^M b_k = D$, $b_k \cap b_l = \emptyset$, for all pairs of blocks b_k and b_l . The vector $w_{b_k} = \{w(s_i); s_i \in b_k\}$ where $\dim(w_{b_k}) = n_k$ such that $\sum_{k=1}^M n_k = n$. Then, we assume that the w_{b_l} and w_{b_j} , for $l \neq j$, are conditionally

independent given some “past” blocks, and the joint density of w_S is approximated by

$$\tilde{p}(w_S) = p(w_{b_1}) \prod_{k=2}^M p(w_{b_k} | w_{N(b_k)}), \quad (2)$$

where $N(b_k) \subset S \setminus [s_i \in b_k]$ is the set of nb neighbor blocks of b_k .

Proposition 1. *Let $G = \{S, \xi\}$ be a chain graph, where $S = \{s_1, \dots, s_n\}$ is the set of nodes, and ξ is comprised by: (i) the set of directed edges from every node in the set $s_{b_k} = \{s_i \in b_k, \forall i = 1, \dots, n\}$, to all nodes in $N(b_k)$, $\forall k = 1, \dots, M$, and (ii) the set of undirected edges between every pair of nodes in b_k . Let G_b be a subgraph of G composed by M nodes, such that each node is one node of the set s_{b_k} . If G_b is acyclic and $p(w_S)$ is a valid multivariate joint density, then $\tilde{p}(w_S)$ in Equation (2) is also a valid multivariate joint density.*

The proof of this proposition and subsequent proofs are found in Appendix A1. A chain graph G , also called partially directed acyclic graphs, is defined by a set of nodes disjointly partitioned into several chain components, edges between nodes in chain are undirected and edge between nodes in different chains are directed. If we take one node per chain they form a directed graph which we call G_b . Proposition 1 states that Equation (2) is a proper multivariate joint density when $p(w_S)$ is a valid multivariate joint density and G is a chain graph which has a directed acyclic graph (DAG) G_b . In particular, if $N(b_k)$ is any subset of $\{N(b_1), \dots, N(b_{k-1})\}$ then G_b is acyclic (Figure (1)). This choice of neighbor sets do not unvalidate the acyclic property between blocks and also produce valid densities. With this choice, we are assuming that $\forall w(s_i); s_i \in b_k$, they are dependent between them, but also that each one depends on $w(s_j) \in w_{N(b_k)}$, that is, depends on the neighbor blocks of b_k . Hence, $w(s_i)$ is explained by all of its nearest neighbors in the block b_k and some nearest neighbor blocks from the past, which avoids loss of information at small scale while preserving information at large scale, respectively. In fact, sometimes when the spatial dependence is strong relative to the spatial domain of observation, it can be advantageous to include some observations in $N(b_k)$ that were rather distant from $s_{b_k} = \{s_i \in b_k, \forall i = 1, \dots, n\}$ (Stein et al., 2004). This situation was not presented in any of Datta et al. (2016) examples. Each $w(s_i)$ depends on $n_{b_k} = n_k - 1 + N_{b_k}$ neighbors, where N_{b_k} is the number of locations in the neighboring blocks of b_k . Further G is sufficiently sparse if n_k and N_{b_k} are sufficiently small. Note that for the NNGP process, each $w(s_i)$ only depends on at most m nearest neighbors from the past such that $m \ll n$. In particular, the NNGP will be a special case of our proposed spatial process (see corollary 3).

Let w_S be a realization of a GP over S with covariance function $C(\theta)$, therefore $p(w_S)$ is the probability density (pdf) of a n -variate normal distribution with mean zero and covariance matrix C_S . From the proposition 1 holds the next corollary.

Corollary 1. *Suppose $p(w_S)$ is the pdf of a n -variate normal distribution with mean zero and covariance matrix C_S . If G is a chain graph and G_b is a DAG, as we specified in proposition 1, then $\tilde{p}(w_S)$ is a proper density.*

From basic properties of normal distributions, $w_{b_k} | w_{N(b_k)} \sim N_n(B_{b_k} w_{N(b_k)}, F_{b_k})$, $B_{b_k} = C_{b_k, N(b_k)} C_{N(b_k)}^{-1}$ and $F_{b_k} = C_{b_k} - C_{b_k, N(b_k)} C_{N(b_k)}^{-1} C_{N(b_k), b_k}$, where $C_{i,j}$ and C_i are elements of C_S .

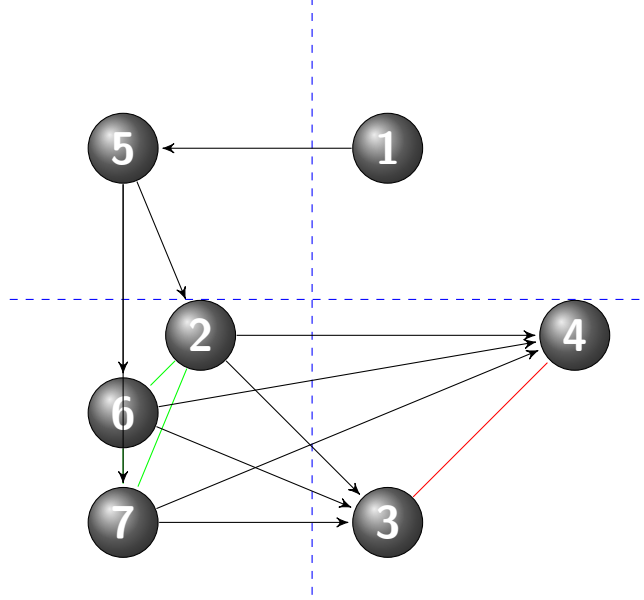


Figure 1: Illustration of a chain graph with $n = 7$ nodes and $M = 4$ blocks: $b_1 = \{1\}$, $b_2 = \{5\}$, $b_3 = \{2, 6, 7\}$, $b_4 = \{3, 4\}$.

Then if f is the pdf of a normal distribution, Equation (2) is defined by

$$\tilde{p}(w_S) = \prod_{k=1}^M f(w_{b_k} | B_{b_k} w_{N(b_k)}, F_{b_k}). \quad (3)$$

Proposition 2. *If $p(w_S)$ is a proper pdf of a n -variate normal distribution with mean zero and covariance matrix C_S , G is a chain graph and G_b is a DAG, as we specified in proposition 1, then*

- (i) $\tilde{p}(w_S)$ is also the pdf of a n -variate normal distribution with mean zero and covariance matrix $\tilde{C}_S = (B_S^T F_S^{-1} B_S)^{-1}$,
- (ii) B_S is a block matrix and a lower triangular matrix,
- (iii) F_S is block diagonal,
- (iv) \tilde{C}_S is positive definite, and
- (v) If $n_{b_k} \ll n; \forall k = 1, \dots, M$ then \tilde{C}_S^{-1} is sparse.

The multivariate normal distribution is completely specified by its expectation which is assumed to be zero, and its covariance function which is valid since it is positive definite from Proposition 2 (iv). In addition, Proposition 2 also states that B_S is a block matrix and F_S is block diagonal, due to these features we are able to implement our algorithm using parallel processing. The sparsity of the precision matrix in fact represents that distant pair of observations, as well as, distant block of observations are independent. Note that if we assume

more blocks, the precision matrix will be more sparse. The reduction in computational complexity is achieved through such sparsity of the precision matrices and we also can parallelize many computations for blocks of data. Then, $\tilde{p}(w_S)$ is a proper multivariate joint density with a sparse precision matrix which enjoys great features, as a result, it is easier to work with $\tilde{p}(w_S)$ than with $p(w_S)$. We remark that $\tilde{p}(w_S)$ is a valid pdf, and we could perform inference directly from a likelihood function not a composite or pseudo-likelihood. For instance, Eidsvik et al. (2014) achieved inference through block-composite likelihood, but their approach ignores information about components of the covariance structure, as a consequence, there is loss of statistical efficiency.

To build a general valid spatial process, we need to provide a pdf consistent with some well-defined random field. Hence, following the NNGP approach, we use $\tilde{p}(w_S)$ to provide such pdf. We also assume that S is a set of fixed and observed locations. And, we define $U = \{u_1, \dots, u_l\}$ as any finite set of locations such that $S \cap U = \emptyset$ and $V = S' \cup U$, $S' \subset S$. Using the conditional distribution properties and corollary 1, we have that the approximated conditional pdf of $p(w_U|w_S)p(w_S)$ defined by $\tilde{p}(w_U|w_S)\tilde{p}(w_S)$ is also a proper density if $\tilde{p}(w_U|w_S)$ is proper. Notice that $p(w_U|w_S)$ is proper since $\{w_U, w_S\}$ is a realization of the $GP(0, C(\theta))$. For simplicity, if we assume that w_{u_i} is independent of w_{u_j} given w_S , then we define $\tilde{p}(w_U|w_S) = \prod_{i=1}^l p(w_{u_i}|w_S)$. Further, if we also assume that w_{u_i} only depends on some observations of w_S , $N(u_i)$, which is the set of neighbors of u in S , then $\tilde{p}(w_U|w_S) = \prod_{i=1}^l p(w_{u_i}|w_{N(u_i)})$ which is proper. Now, we assume that $w_U|w_S$ follows a multivariate normal distribution with the following pdf, $\tilde{p}(w_U|w_S) = \prod_{i=1}^l f(w_{u_i}|B_{u_i}w_{N(u_i)}, F_{u_i})$, where $B_{u_i} = C_{u_i, N(u_i)}C_{N(u_i)}^{-1}$ and $F_{u_i} = C_{u_i} - C_{u_i, N(u_i)}C_{N(u_i), u_i}^{-1}C_{N(u_i), u_i}$, $C_{i,j}$ and C_i are elements of C_S .

Then we can define an approximation of the pdf $p(w_V)$ as follows,

$$\tilde{p}(w_V) = \int \tilde{p}(w_U|w_S)\tilde{p}(w_S) \prod_{s_i \in (S')^c} d(w(s_i)), \quad (4)$$

where $(S')^c$ is the complement of S' and $\tilde{p}(w_V)$ is a proper density for any choice of $N(u_i)$. Katzfuss and Guinness (2017) proposed a general Vecchia approximation, which is very similar in form to the pdf $\tilde{p}(w_V)$, if we assume $S = S'$, they proved that such approximation yields a joint multivariate distribution. Their most similar case assumes a similar $\tilde{p}(w_S)$, using vectors of observations, but we define $\tilde{p}(w_U|w_S)$ different from their approach to build a valid spatial process. We prove that the joint distribution of w_V is consistent with some well-defined stochastic process, in the sense that the Kolmogorov's consistency conditions are verified, that is, if the symmetry and compatibility conditions hold for the process defined through the finite-dimensional distributions in Equation (4). For this reason we need to be careful when defining $\tilde{p}(w_U|w_S)$ to ensure that it will be the same under reordering of the sites.

Lemma 1. *Let $\tilde{p}(w_V)$ in Equation (4) be a pdf, where S is fixed, w_{u_i} given $w_{N(u_i)}$ is independent of w_{u_j} given $w_{N(u_j)}$, for $N(u_i) = \{s_{b_j} \in S, u_i \in b_j\} \forall i = 1, \dots, l$ and proper normal densities $\tilde{p}(w_{u_i}|w_{N(u_i)})$. Then the finite-dimensional distributions with pdf $\tilde{p}(w_V)$ support a valid random field w_V for all $V \subset \mathbb{R}^2$, that is, they satisfy the Kolmogorov's conditions of symmetry and consistency.*

Following the NNGP we could have chosen $N(u_i)$ to be the m nearest neighbors of u_i in S . Nevertheless, henceforth $N(u_i)$ comprises the observed locations in the block where u_i

belongs in the spatial domain D , therefore, $N(u_i)$ depends on the same observations in S for any order of U . Hence, lemma 1 defines a new valid spatial process and the next theorem proves that such spatial process derived from a GP is also a GP.

Theorem 1. *For any finite set $V \in D$, $\tilde{p}(w_V)$ in Equation (4) is the finite dimensional density of a Gaussian process, called block-NNGP, with cross covariance function*

$$\tilde{C}_{v_i, v_j} = \begin{cases} \tilde{C}_{s_i, s_j} & \text{if } (v_1 = s_i, v_2 = s_j) \in S \\ B_{v_1} \tilde{C}_{N(v_1), s_j} & \text{if } v_1 \notin S \text{ and } v_2 = s_j \in S \\ \delta_{(v_1=v_2)} F_{v_1} + B_{v_1} \tilde{C}_{N(v_1), N(v_2)} B_{v_2}^T & \text{if } (v_1, v_2) \notin S, \end{cases}$$

where $\tilde{C}_{m,n}$ is the covariance matrix of \tilde{C}_S .

The block-NNGP contains existing processes as special cases. If we consider one observation per block and nb is the number of “past” nearest neighbor observations, the NNGP with S being the set of all observed locations is a particular case of block-NNGP. Also when $N(b_k) = \emptyset, \forall k$ each block $w_{N(b_k)}$ is independent from the other blocks, that is, $w_{N(b_k)} \perp w_{N(b_j)}, \forall k \neq j$, and we say that the spatial process is composed by independent blocks (Stein, 2013).

Corollary 2. *The block-NNGP with $M = n$ and $nb = m$ recovers the NNGP when S is the set of all observed locations.*

Corollary 3. *The block-NNGP with M blocks and $nb = 0$ recovers the independent blocks approach.*

Following previous blocking strategies (Kim et al., 2005; Eidsvik et al., 2014), the spatial domain can be partitioned into several regions, either using a regular block design (Figure (2)a) or an irregular block design (Figure (2)b). If the observed locations are approximately uniformly distributed over the domain D , the partitions can simply be obtained by splitting the spatial domain into M subregions of approximately equal area. If the observation locations are far from uniform, more complicated partitioning schemes might be necessary to achieve fast inference. In our approach, for the regular block design we fixed the number of blocks, and each block can have different number of observations. While for the irregular block design, we have fixed the number of observations per block. Of course, different block designs can also be implemented, for instance Voronoi/Delaunay designs (Eidsvik et al., 2014).

3 Bayesian estimation for block-NNGP

Let $Y = (Y(s_1), \dots, Y(s_n))$ be a realization of a spatial stochastic process defined for all $s_i \in D \subset \mathbb{R}^2, i = 1, \dots, n$. The basic geostatistical Gaussian regression model is of the form

$$Y(s_i) = X'(s_i)\beta + w(s_i) + \epsilon(s_i),$$

where β is a coefficient vector (or regression parameter), X is a vector of covariates, $w(s)$ is a spatial structured effect, it captures the spatial association, and $\epsilon(s_i) \sim N(0, \tau^2)$

models the measurement error. Thus, $y|\beta, w, \tau^2 \sim N(X\beta + w, D(\tau^2))$, where D is a diagonal matrix with entries τ^2 . Full Bayesian specification is available if we assign priors to β, w, τ , and hyperparameters. Hence, instead of the Gaussian process prior for w , we assume that $w \sim \text{block-NNGP}(0, \tilde{C}(\theta))$, and we also assume $\beta \sim N(\mu_\beta, V_\beta)$ and $\theta^* = (\phi, \sigma^2, \tau^2) \sim \pi(\theta^*)$. So, the joint posterior distribution is given by

$$p(\theta^*, \beta, w|y) \propto p(\theta^*) \times p(\beta|\mu_\beta, \Sigma_\beta) \times p(w|0, \tilde{C}(\theta)) \times p(y|X\beta + w, D(\tau^2)). \quad (5)$$

In particular, assuming that $S = \{s_1, \dots, s_n\}$ is the set of locations where the outcomes have been observed and $S' = S$, then for estimation we have that $w = w_S$ and $\tilde{C}(\theta) = \tilde{C}_S(\theta)$ in Equation (5).

The Markov Chain Monte Carlo (MCMC) implementation usually requires updating the n latent spatial effects w sequentially, in addition to the regression and covariance parameters (for instance, see Datta et al. (2016)). Finley et al. (2017) studied the convergence for very large spatial datasets using NNGP to prove that such sequential updating of the random effects often leads to very poor mixing in the MCMC. To overcome this issue they proposed the Collapsed MCMC NNGP, which in summary performs Gibbs Sampling and random walk Metropolis steps to update β and θ , respectively, and then recover w and predictions y_0 using composition sampling.

The Collapsed MCMC for block-NNGP follows the steps: (i) update θ^* through Random walk Metropolis-Hastings (MH). The target log-density is $p(\theta^*|y) \propto p(\theta^*) \times N(y|X\beta, \Sigma_{y|\beta, \theta})$; where $\Sigma_{y|\beta, \theta} = \tilde{C}_S + D$; (ii) Gibbs's sampler update for β , from the full conditional $\beta|y \sim N(Bb, B)$ where $B = (\Sigma_\beta^{-1} + X^T \Sigma_{y|\beta, \theta}^{-1} X)^{-1}$ and $b = \Sigma_\beta^{-1} \mu_\beta + X^T \Sigma_{y|\beta, \theta}^{-1} y$; (iii) Recover $w_S|\theta^*, \beta$ for each post-burn in MCMC sample; $w_S|\beta, \theta^*, y \sim N(Ff, F)$, where $F = (\tilde{C}_S^{-1} + D^{-1})^{-1}$ and $f = D^{-1}(y - X\beta)$.

Spatial prediction can be carried out after parameter inference. Conditioning on a particular estimated value of the parameters (θ, β) , spatial prediction amounts to finding the posterior predictive distribution at a set of prediction locations u_i , that is, $p(y(u_i)|y)$. Note that we consider all observed data for estimation, thus S comprises the observed locations, while the new location points for predictions belong to the finite set U . Furthermore, since the components of $w_U|w_S$ are independent, we can update $w(u_i)$ for each $i = 1, \dots, l$, from $p(w(u_i)|w_S, \beta, \theta^*, y) \sim N(m, v)$, where $m = C_{u_i, N(u_i)}^T C_{N(u_i), N(u_i)}^{-1} w(N(s_0))$ and $v = \sigma^2 - C_{u_i, N(u_i)}^T C_{N(u_i), N(u_i)}^{-1} C_{u_i, N(u_i)}$. Block NNGP are especially useful here as posterior sampling for w_U is cheap because their components are independent and each $w(u_i)$ is only based on the observations that lie in the block that it belongs. Now using the posterior samples of $w(u_i)$, the posterior predictive sampling $y(u_i)|w_U, w_S, \beta, \theta^*, y \sim N(X(u_i)^T \beta + w(u_i), \tau^2)$.

Our approach does not need to store $n \times n$ dense distance matrices, it stores M "small" dense matrices. It is scalable to massive datasets, we can compute the precision matrix from the block-NNGP using faster (parallel) computation for the defined blocks. For shared Memory, good parallel libraries are available, such as the multi-threaded BLAS/LAPACK libraries included in Microsoft R Open and parallel Packages in R like the doMC Package (Calaway et al., 2017).

4 Simulation Studies

To assess the performance of the block-NNGP models, we present the next simulation experiments. We generate a spatial process with $n = 2500$ observation sites on a spatial domain $(0, 1) \times (0, 1)$. The covariates are $X(s_i) = (1, x_i)$, $x_i \sim (N(0, 1))$ with true regression parameters $\beta = (1, 5)^T$. We use an exponential covariance function $C(h) = \sigma^2 \exp(-\|s_i - s_j\|)$ with $\sigma^2 = 1$. The so-called effective range (r), the distance at which the correlation decays to 0.1, is studied using simulation scenarios, (i) SIM I: $r = 0.16$ ($\phi = 12$) (ii) SIM II: $r = 0.33$ ($\phi = 6$), and (iii) SIM III: $r = 0.67$ ($\phi = 3$), where $\phi = \sqrt{(8 \times \nu)/range}$ (with $\nu = 0.5$) is called the spatial decay. For all locations we considered $\tau^2 = 0.1$.

Let S be the set of $n = 2000$ observed locations and U the set of the remaining 500 observations used to assess predictive performance. We fit the models: (i) full Gaussian process (full GP), (ii) block-NNGP models with $M = n$ for $nb = 10$ and $n = 20$, which by Corollary 4.1 is equivalent to the NNGP model with 10 and 20 neighbors respectively, (iii) regular (R) block-NNGP models and (iv) irregular (I) block models. We vary the number of spatial blocks to investigate the way blocking schemes influence the estimation and prediction capabilities. We use regular blocks and irregular blocks (Figure (S1)). The regular blocks have the same size. The number of blocks $M = n_m \times n_m$, for instance, $3^2, 5^2, 7^2$, and 10^2 . A similar configuration was also used in Eidsvik et al. (2014). Our irregular blocks design requires grouping approximately n/M observations per block, so the region D is subdivided into M irregular regions. In the regular case, we are also able to know the number of observations per block (n_k), but our main concern comes when the observed locations are not uniformly distributed over the domain D because the (n_k) will be very different for each block k , and for some blocks it will be expensive to perform matrix operations. On the other hand, with irregular blocks we can control the approximated number of observations per block and the sparsity of \tilde{C}_S^{-1} (Figure (S2)). In both cases the maximum number of blocks should be constrained by some prior information about the range of the process. Although there might not be an explicit number of blocks and neighboring blocks for optimal blocking, we will determine them by the computational speed as well as statistical efficiency, maximizing the number of blocks.

The parameters of the models are estimated from a Bayesian point of view, so we run the MCMC for a small number of iterations (1000) to determine the “best” number of blocks in terms of less time. Figure (2) shows that for this configuration and different values of ϕ , the time does not significantly decrease for $M > 9^2$. We also test Widely Applicable Information Criterion (WAIC, Watanabe, 2010) and logarithm of the pseudo-marginal likelihood (LPML, Dey et al., 1997) to study the goodness of fit for different number of blocks and neighbor blocks, but we did not get any pattern. Then full posterior inference for subsequent analysis was based upon one chain of 25000 iterations (with a burn-in of 5000 iterations). In particular, the collapsed MCMC method (Finley et al., 2017) was adapted to the block-NNGP. We use flat prior distributions for β , for σ^2 we assigned inverse Gamma $IG(2, 1)$ prior, for τ^2 we assigned $IG(2, 0.1)$ prior, and for the spatial decay ϕ we assigned a uniform prior $U(2, 30)$ which is equivalent to a range between approximately 0.067 and 1 units. We also used a parameterization on the real line, with log variance, log precision and log range parameters.

Parameter estimates and performance metrics for the models proposed when $\phi = 12$

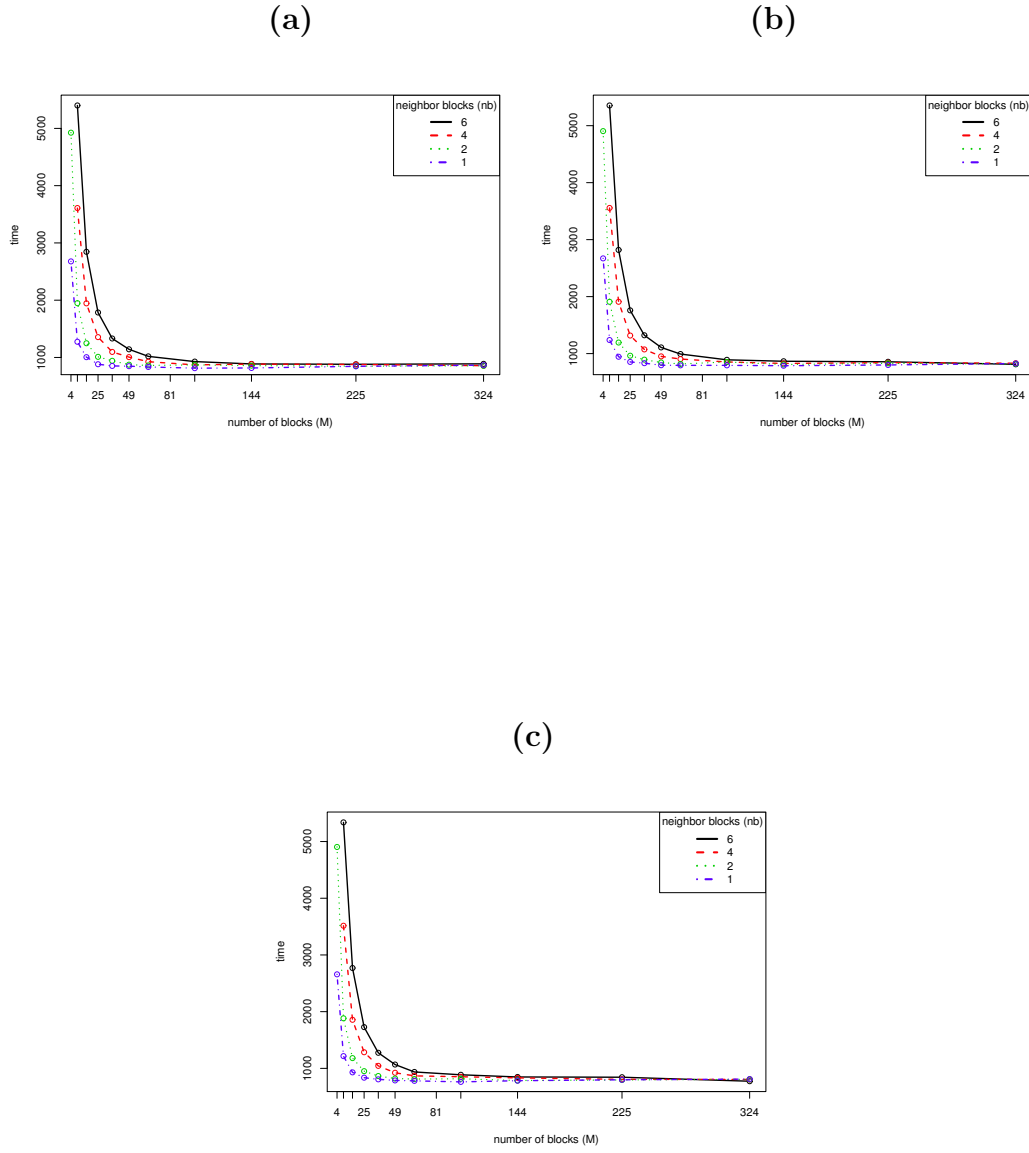


Figure 2: MCMC time for block-NNGP models running 1000 iterations, for regular blocks.
(a) SIM I ($\phi = 12$), (b) SIM II ($\phi = 6$) and (c) SIM III ($\phi = 3$).

Table 1: SIM I ($\phi = 12$) Summary of mean parameter estimates. Parameter posterior summary (2.5, 97.5) percentiles.

Model		Full GP	NNGP (20)	NNGP (10)	(R)M=100 nb=1	(R)M=64 nb=1	(I)M=100 nb=1	(I)M=200 nb=2
σ^2	1	0.99 (0.79, 1.36)	1.07 (0.91, 1.47)	1.04 (0.89, 1.32)	1 (0.83, 1.31)	0.99 (0.81, 1.27)	0.92 (0.78, 1.12)	0.94 (0.77, 1.18)
τ^2	0.1	0.1 (0.08, 0.12)	0.09 (0.07, 0.11)	0.09 (0.07, 0.11)	0.1 (0.08, 0.12)	0.1 (0.08, 0.12)	0.1 (0.08, 0.12)	0.1 (0.08, 0.12)
ϕ	12	13.74 (9.48, 17.74)	13.09 (9.08, 14.93)	13.64 (10.2, 14.91)	13.52 (9.87, 16.95)	13.6 (10.15, 17.38)	14.79 (11.67, 17.98)	14.22 (10.56, 17.86)
β_0	1	1.09 (0.79, 1.49)	1.18 (0.85, 1.61)	0.98 (0.67, 1.29)	1.12 (0.91, 1.37)	1.12 (0.89, 1.39)	0.72 (0.52, 0.91)	0.92 (0.69, 1.19)
β_1	5	5.01 (4.99, 5.03)	5.01 (4.99, 5.03)	5.01 (4.99, 5.03)	5.01 (4.99, 5.04)	5.01 (4.98, 5.03)	5.01 (4.99, 5.04)	5.01 (4.99, 5.03)
LPML		-31084.36	-35783.45	-36204.53	-30747.6	-30260.92	-30245.45	-29973.36
WAIC2		184256.5	228406.8	232569.2	181016	176769.5	176363.1	174723.1
G		66.46808	58.47473	57.72994	65.74294	67.48258	66.19069	69.10049
P		329.3224	304.9878	303.4614	335.6308	338.47	340.2987	337.6664
D		395.7905	363.4625	361.1913	401.3738	405.9526	406.4894	406.7669
RMSPE		—	0.562189	0.5506445	0.5674386	0.5875377	0.5636098	0.5569855
Accep		23.73333	34.45	35.74	23.13333	23.63	23.36333	23.69333
time (sec)		31637.95	23915.9	23357.57	23758.02	24683.79	22990.89	22915.74

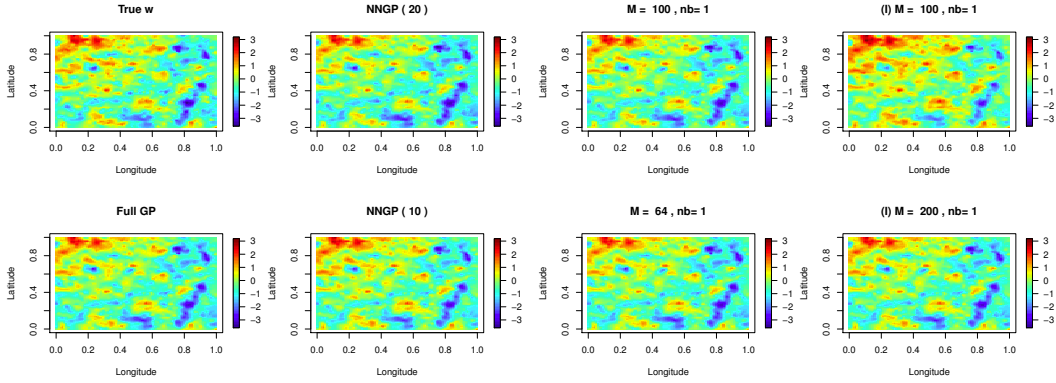


Figure 3: SIM I ($\phi = 12$). True spatial random effects and posterior mean estimates for different models.

are provided in Table (1). In all cases, the mean posterior estimates for block-NNGP are very close to the full-GP mean posterior estimates. The goodness of fit and predictive performance for all models are very similar. The number of neighbors of block-NNGP models with irregular blocks ($n_{bk} = 40 - 1$ for $M = 100, nb = 1$ and $n_{bk} = 30 - 1$ for $M = 200, nb = 2$) is higher than the number of neighbors of NNGP models (10 and 20). Nevertheless these block-NNGP models are faster and they also show a slightly better performance to fit the data, thus it has more information about the process without increasing the computational cost. In fact, Figure (3) shows the similarity of estimations of w_S , interpolated over the domain, between all block-NNGP models and Full GP. We conclude that for this simulated data we detect no differences between the block-NNGP models, and they fit the data very well when the range is very small.

To study the statistical efficiency when the effective correlation length increases, while keeping the domain fixed, we evaluate the performance of the proposed models when $\phi = 6$. In Table (2), it is observed that estimations of the block-NNGP models closely approximate

Table 2: SIM II ($\phi = 6$) Summary of mean parameter estimates. Parameter posterior summary (2.5, 97.5) percentiles, $n = 2000$.

Model		Full GP	NNGP (20)	NNGP (10)	(R)M=64 nb=1	(R)M=144 nb=6	(I)M=100 nb=2	(I)M=100 nb=1
σ^2	1	1.35 (0.83, 2.12)	1.72 (1.01, 2.31)	1.01 (0.74, 1.66)	1.38 (0.95, 2.05)	1.08 (0.75, 1.93)	1.06 (0.78, 1.12)	0.96 (0.75, 1.31)
τ^2	0.1	0.14 (0.09, 0.12)	0.1 (0.08, 0.12)	0.1 (0.08, 0.11)	0.11 (0.09, 0.12)	0.1 (0.09, 0.12)	0.11 (0.09, 0.12)	0.11 (0.09, 0.12)
ϕ	6	4.93 (3.14, 8.17)	3.88 (3.03, 6.96)	6.91 (4.03, 9.87)	4.67 (3.11, 7.04)	6.26 (3.35, 9.28)	6.2 (3.75, 8.75)	6.85 (4.76, 9.07)
β_0	1	1.5 (0.77, 2.67)	1.97 (1.05, 3.23)	0.87 (0.36, 1.42)	1.43 (0.93, 2.16)	1.11 (0.55, 1.91)	1.03 (0.57, 1.7)	0.61 (0.31, 0.94)
β_1	5	5.01 (4.99, 5.03)	5.01 (4.99, 5.03)	5.01 (4.99, 5.03)	5.01 (4.99, 5.03)	5.01 (4.99, 5.03)	5.01 (4.99, 5.03)	5.01 (4.99, 5.03)
LPML		-26101.92	-27891.44	-29292.24	-24944.26	-26345.72	-25364.79	-25435.02
WAIC2		146979.3	161696.3	173963.3	137423.1	148797.4	140935.4	140785.8
G		98.60967	94.5057	89.47476	101.9886	97.27277	100.5962	98.87815
P		313.3962	303.9089	298.1956	324.1011	312.4023	319.8328	324.3391
D		412.0059	398.4146	387.6703	426.0897	409.6751	420.429	423.2173
RMSPE		—	0.7678724	0.4926092	0.5830725	0.5996594	0.5310345	0.4934768
Accep		28.69	32.61333	28.59	29.14	26.50333	26.19	25.17333
time (sec)		31677.58	23896.63	23423.89	23840.58	24166.43	23867.53	22746.49

to the ones of full GP model. Figure (4) shows the posterior mean estimates of the spatial random effects interpolated over the domain. As illustrated in Figure (4), the block-NNGP models can result in considerably better approximations, specially for $M=225$ and $nb = 2$. The LPML and WAIC values suggest that the block-NNGP models are the best to fit the data. Computing times requirements for NNGP and block-NNGP models are similar, but as we expected lower than the full GP model time.

Further comparisons show that the mean posterior estimates of σ^2 , ϕ and β_0 for the NNGP model with 20 neighbors and full GP are a little different (Table (2)). We might think that if we increase the number of neighbors, the estimation of parameters using the NNGP model should be better, but this is not guaranteed as we can see from this simulation. In fact, Figure (4) also shows that the NNGP model with 20 neighbors did not approximate well the spatial field of the full GP model. The patterns differ greatly from the original spatial random field and the one estimated using the full-GP. Otherwise the block-NNGP model with $M = 64$ and $nb = 1$ has bigger blocks but the estimation is improved without increasing the computing time requirements drastically. So, although the NNGP has proven to be successful in capturing local/small-scale variation of spatial processes, it might have one disadvantage: inaccuracy in representing global/large scale dependence. This might happen because the NNGP built the DAG based on observations, where the locations are ordered by one of the coordinates. Adversely, the block-NNGP chain graph is based on blocks of observations, which captures both small and large dependence.

Table (3) provides parameter estimates and performance metrics for all models when $\phi = 3$. It is observed that estimations of the block-NNGP models closely approximate to the ones of full GP model, except the block-NNGP model with $M = 100$ and $nb = 1$. Figure (5) shows the posterior mean estimates of the spatial random effects interpolated over the domain. We can see that the block-NNGP models result in considerably better approximations, specially for $M = 225$ and $nb = 2$. The LPML and WAIC values support also this statement. Computing times requirements for NNGP and block-NNGP models are similar.

Further comparisons show that mean posterior estimates of β_0 for NNGP and full GP

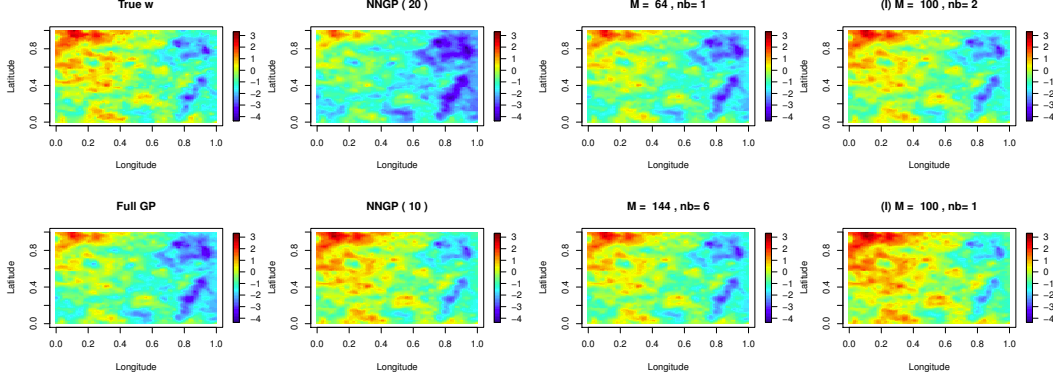


Figure 4: SIM II ($\phi = 6$). True spatial random effects and posterior mean estimates for different models.

are a little different (Table (3)). Figure (5) shows that the spatial random effects with 20 neighbors is too smooth. Also we can see that the map for the NNGP-model and the block-NNGP model with $M = 100$ and $nb = 1$ are very similar to the true process, but different of the full GP model. In NNGP and the block-NNGP models the number of neighbors is small, so we might think that if we increase the number of neighbors, the estimation of parameters using the NNGP model should be better, but this is not guaranteed as we can see from simulation with $\phi = 6$. And if we use more neighbors than the “necessary” the model oversmooth the spatial process. In general, if the block-NNGP models has more neighbors per observation, that is more neighboring blocks, the block-NNGP process is more similar to the GP Full process without increasing the computing time requirements drastically.

Table 3: SIM III ($\phi = 3$): Summary of mean parameter estimates. Parameter posterior summary (2.5, 97.5) percentiles, $n = 2000$.

Model		Full GP	NNGP (20)	NNGP (10)	(R)M=225 nb=2	(R)M=324 nb=2	(I)M=100 nb=1	(I)M=200 nb=2
σ^2	1	1.37 (0.86, 1.79)	2.65 (1.36, 3.55)	1.12 (0.66, 2.68)	2.03 (0.97, 3.07)	2.37 (1.38, 3.21)	0.97 (0.69, 1.65)	1.98 (0.96, 1.04)
τ^2	0.1	0.1 (0.09, 0.12)	0.1 (0.09, 0.12)	0.1 (0.09, 0.12)	0.11 (0.1, 0.12)	0.11 (0.1, 0.12)	0.11 (0.1, 0.12)	0.11 (0.1, 0.12)
ϕ	3	2.41 (2.01, 3.97)	1.25 (1.01, 2.48)	3.03 (1.22, 5.46)	1.48 (1.03, 3.17)	1.26 (1.01, 2.22)	3.22 (1.76, 4.7)	1.54 (1.04, 3.33)
β_0	1	1.95 (0.85, 3.27)	3.09 (1.29, 5.33)	0.8 (-0.18, 1.83)	1.55 (0.35, 3.16)	1.81 (0.44, 3.39)	0.67 (0.2, 1.25)	1.73 (0.68, 3.29)
β_1	5	5.01 (4.99, 5.03)	5.01 (4.99, 5.03)	5.01 (4.99, 5.03)	5.01 (4.99, 5.03)	5.01 (4.99, 5.03)	5.01 (4.99, 5.03)	5.01 (4.99, 5.03)
LPML		-21883.68	-22780.12	-23219.55	-20010.68	-20096.75	-20784.85	-21050.7
WAIC2		115927.4	122610.6	126136.8	102370.9	102763.3	107298.9	110547.8
G		127.6543	126.3956	123.6112	138.2599	137.6801	132.412	132.6907
P		291.0201	285.967	285.0954	299.7904	300.6322	303.5624	295.7998
D		418.6744	412.3627	408.7066	438.0503	438.3123	435.9745	428.4904
RMSP		—	1.077448	0.5020536	0.8271246	0.8799603	0.4356712	0.8119286
Accep		32.72667	32.31667	24.49	30.09667	32.02	23.82	29.16667
time (sec)		32814.86	23061.93	23760.52	23284.51	24529.85	23973.31	23912.96

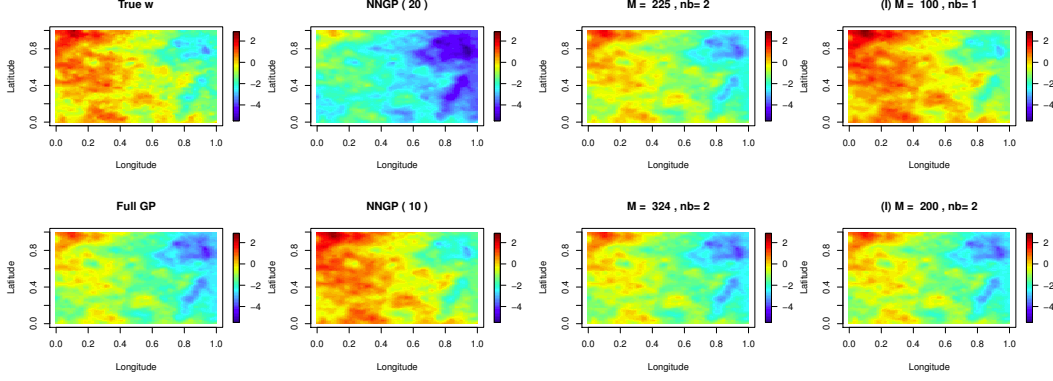


Figure 5: SIM III ($\phi = 3$). True spatial random effects and posterior mean estimates for different models.

5 Application

In this section, we illustrate the application of block-NNGP to large spatial data from the mining industry. In the process of extracting ore, stability is crucial because it is one of the key characteristics that influence the success of underground mining work. If it is not possible to produce ore above cut-off at stable conditions, the ore is made inaccessible, which often results in lost production. To assess the stability of the rock mass it is studied the spatial joint frequency distribution in a mine because a joint is a planar or semiplanar discontinuity in a rock mass and represents zones of weakness in the rock mass (Ellefmo and Eidsvik, 2009).

Here we study joint-frequency data in an iron mine in the northern part of Norway to estimate the most probable joint frequency at unsampled locations. Eidsvik et al. (2014) aggregated the raw joint data along the boreholes, thus we have the total number of 11,701 measurements. Then they transformed the data, the logarithm of the joint-frequency observations are standardized. In Figure (6), we display locations of the measurements (east, north) of the joint-frequency data. The depth of boreholes is used as covariate, along with an intercept. More references about these data can be found in (Ellefmo and Eidsvik, 2009) and Eidsvik et al. (2014).

We first divide the joint-frequency data in two subsets, the set S composed by a random subset of 11000 observed locations and the remaining 701 observations were withheld to assess predictive performance, so they belong to the set U . We fit the block-NNGP models with different number of regular blocks and different neighboring blocks. We only run the MCMC for 1000 iterations to choose between these models, thus we choose the model with $M = 289$ blocks and $nb = 1$ block (Figure (6)). Then full Bayesian inference and posterior inference were based upon 10000 iterations. We use flat prior distributions for β , vague priors for σ^2 and for τ^2 which were an inverse Gamma $IG(2, 1)$ and $IG(2, 0.1)$ respectively, and for the spatial decay ϕ we assigned a uniform prior $U(0.001, 2)$ which is equivalent to a range between approximately 1 and 2000m.

From the parameter estimates, the mean effective spatial range is approximately 29m

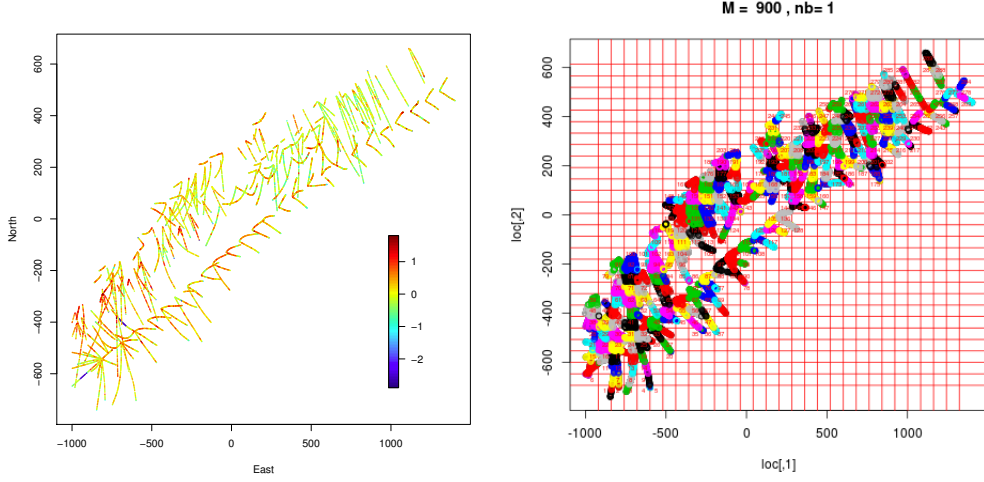


Figure 6: Left: Joint-frequency data, $n = 10701$ locations. Right: Regular blocks for these data.

($\phi = 0.07$), the nugget effect equal to 0.1 and the marginal variance equal to 0.16. These results are very similar to the parameter estimates of block composite likelihood proposed by Eidsvik et al. (2014) using a Matérn covariance function with $\nu = 3/2$. Figure (7) shows a maps of posterior estimates for the spatial random effect and interpolated posterior predictive mean of joint-frequency data. Comparing to Figure (6), it is easy to see that our estimations are rather accurate.

6 Discussion

We have presented the block-NNGP, a new GMRF for approximating Gaussian processes with any covariance function. The precision matrix of the block-NNGP has a block-sparse structure, which allows scalable inference and distributed computations. It is one of the methods in the state-of-the-art for large spatial data and can be viewed as a general case of the NNGP (with $M = n$) of Datta et al. (2016). The results for block-NNGP and NNGP are very similar for small ranges of the spatial random field. In addition, it improves the NNGP when the range is not too small.

Using theoretical results, a toy example, large simulated datasets, and a real-data application, we have shown that the block-NNGP can provide a better approximation at the same or lower computational complexity and computation time. It should also be noted that our inference results for $M \neq n$ provide an algorithm for parallel blocks and distributed computations for inference. The block-NNGP not only approximates the data precision matrix to a sparse precision matrix, but it is also a valid Gaussian process in its own right. Extensions to more complicated scenarios are therefore possible by assuming different sets S and U , or chain graphs. Finally, we remark that a more sophisticated implementation would allow more speed-up for the block-NNGP model, using a parallel for-loop and running matrix decompositions in parallel. This is future work.

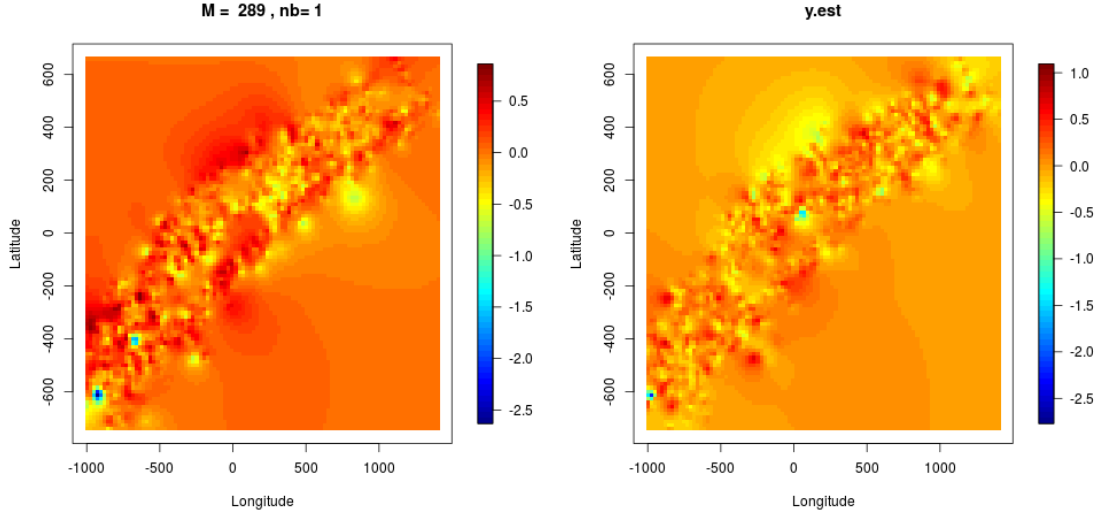


Figure 7: Left: Mean Posterior of w_S . Right: Mean posterior of joint-frequency data.

Acknowledgments

The first author would like to thank ProUNI, and the second author would like to thank FAPEMIG and CNPq, for partial financial support.

References

- Bolin, D. and Wallin, J. (2016). Spatially adaptive covariance tapering. *Spatial Statistics*, 18(Part A):163 – 178.
- Calaway, R., Analytics, R., and Weston, S. (2017). *doMC: Foreach Parallel Adaptor for "parallel"*.
- Caragea, P. C. and Smith, R. L. (2007). Approximate likelihoods for spatial processes. In *Joint Statistical Meetings - Section on Statistics & the Environment*.
- Datta, A., Banerjee, S., Finley, A. O., and Gelfand, A. E. (2016). Hierarchical nearest-neighbor Gaussian process models for large geostatistical datasets. *Journal of the American Statistical Association*, 111(514):800–812.
- Dey, D. K., Chen, M. H., and Chang, H. (1997). Bayesian approach for nonlinear random effects models. *Biometrics*, 53:1239–1252.
- Eidsvik, J., Shaby, B. A., Reich, B. J., Wheeler, M., and Niemi, J. (2014). Estimation and prediction in spatial models with block composite likelihoods. *Journal of Computational and Graphical Statistics*, 23(2):295–315.
- Ellefmo, S. and Eidsvik, J. (2009). Local and spatial joint frequency uncertainty and its application to rock mass characterisation. *Rock mechanics and rock engineering*, 42(4):667688.

- Finley, A. O., Datta, A., Cook, B. C., Morton, D. C., Andersen, H. E., and Banerjee, S. (2017). Applying nearest neighbor Gaussian processes to massive spatial data sets: Forest canopy height prediction across Tanana Valley Alaska. Technical report.
- Guinness, J. (2018). Permutation and grouping methods for sharpening gaussian process approximations. *Technometrics*, 60(4):415–429.
- Henderson, H. V. and Searle, S. R. (1981). The vec-permutation matrix, the vec operator and kronecker products: A review. *Linear and multilinear algebra*, 9(4):271–288.
- Katzfuss, M. and Guinness, J. (2017). A general framework for vecchia approximations of gaussian processes. *arXiv preprint arXiv:1708.06302*.
- Kim, H.-M., Mallick, B. K., and Holmes, C. C. (2005). Analyzing nonstationary spatial data using piecewise gaussian processes. *Journal of the American Statistical Association*, 100(470):653–668.
- Lindgren, F., Rue, H., and Lindström, J. (2011). An explicit link between Gaussian fields and Gaussian Markov random fields: The SPDE approach. *Journal of the Royal Statistical Society. Series B. Statistical Methodology*, 73(4):423–498.
- Rue, H. and Tjelmeland, H. (2002). Fitting Gaussian Markov random fields to Gaussian fields. *Scandinavian Journal of Statistics*, 29((1)):31–50.
- Stein, M. L. (2013). Statistical properties of covariance tapers. *Journal of Computational and Graphical Statistics*, 22(4):866–885.
- Stein, M. L., Chi, Z., and J. Welty, L. (2004). Approximating likelihoods for large spatial data sets. *Journal of the Royal Statistical Society, Series B*, 66(2):275–296.
- Vecchia, A. V. (1988). Estimation and model identification for continuous spatial processes. *Journal of the Royal Statistical Society. Series B (Methodological)*, 50(2):297–312.
- Watanabe, S. (2010). Asymptotic equivalence of bayes cross validation and widely applicable information criterion in singular learning theory. *Journal of Machine Learning Research*, 11:3571–3594.
- Whittle, P. (1954). On stationary processes in the plane. *Biometrika*, 44:434–449.

Appendix

A: Proofs of main results

Proof of Proposition 1. If $p(w_S)$ is a valid multivariate joint density, $p(w_{b_k}|w_{N(b_k)})$ is also proper, and we have that $\int p(w_{b_k}|w_{N(b_k)})dw_{b_k} = 1, \forall k = 1, \dots, M$.

From the definitions of G and G_b there exists a set of nodes $s_{\pi(b_1)}$ in G , such that “the last node” from a DAG G_b belongs to $s_{\pi(b_1)}$. Then the nodes in $s_{\pi(b_1)}$ do not have any directed

edge originating from them. As consequence, any node in block $\pi(b_1)$ can not belong to the set of nodes of any other block. So the term in Equation (2) where all locations of $\pi(b_1)$ appear is $p(w_{\pi(b_1)}|w_{N(\pi(b_1))})$. Using Fubini's theorem, we can interchange the product and integral, thus

$$\begin{aligned} \int p(\tilde{p}(w_S))dw_S &= \int \cdots \int \prod_{i=1}^M p(w_{\pi(b_i)}|w_{N(\pi(b_i))})dw_{\pi(i)} \\ &= \int \cdots \int \prod_{i=2}^M p(w_{\pi(b_i)}|w_{N(\pi(b_i))})dw_{\pi(i)}. \end{aligned}$$

Then, removing any node of $\pi(b_1)$ from G and G_b , we have the chain graph G' and DAG G'_b , respectively. There exists another set of nodes $s_{\pi(b_2)}$ in G' , such that “the last node” from a DAG G'_b belongs to $s_{\pi(b_2)}$. Then the nodes $s_{\pi(b_2)}$ do not have any directed edge originating from them. As consequence, any node in block $\pi(b_2)$ can not belong to the set of nodes of any other block. So the term in Equation (2) where all locations of $\pi(b_2)$ appear is $p(w_{\pi(b_2)}|w_{N(\pi(b_2))})$. Applying the Fubini's theorem again,

$$\int p(\tilde{p}(w_S))dw_S = \int \cdots \int \prod_{i=3}^M p(w_{\pi(b_i)}|w_{N(\pi(b_i))})dw_{\pi(i)}.$$

In a similar way, we find $s_{\pi(b_3)}, \dots, s_{\pi(M)}$, such that,

$$\int p(\tilde{p}(w_S))dw_S = \int \prod_{i=1}^M p(w_{\pi(b_i)}|w_{N(\pi(b_i))})dw_{\pi(i)} = 1. \quad \square$$

Matrix Analysis Background

Theorem A1: A matrix $B \in \mathbb{R}^{m \times n}$ is full column rank if and only if $B^T B$ is invertible

Theorem A2: The determinant of an $n \times n$ matrix B is 0 if and only if the matrix B is not invertible.

Theorem A3: Let T_n be a triangular matrix (either upper or lower) of order n . Let $\det(T_n)$ be the determinant of T_n . Then $\det(T_n)$ is equal to the product of all the diagonal elements of T_n , that is, $\det(T_n) = \prod_{k=1}^n (a_{kk})$.

Proposition A1: If B is positive definite (p.d.), then if S has full column rank, then $S^T B S$ is positive definite.

Corollary A1: If B is positive definite, then B^{-1} is positive definite.

Proof of Proposition 2. Without loss of generality, assume that the data were reordered by blocks. From known properties of Gaussian distributions, $w_{b_k}|w_{N(b_k)} \sim N(B_{b_k} w_{N(b_k)}, F_{b_k})$, where $B_{b_k} = C_{b_k, N(b_k)} C_{N(b_k)}^{-1}$ and $F_{b_k} = C_{b_k} - C_{b_k, N(b_k)} C_{N(b_k)}^{-1} C_{N(b_k), b_k}$. Hence,

$$\begin{aligned} \tilde{p}(w) &= \prod_{k=1}^M p(w_{b_k}|w_{N(b_k)}) \\ &\propto \prod_{k=1}^M \frac{1}{|F_{b_k}|^{1/2}} \exp \left\{ -\frac{1}{2} (w_{b_k} - B_{b_k} w_{N(b_k)})^T F_{b_k}^{-1} (w_{b_k} - B_{b_k} w_{N(b_k)}) \right\} \\ &\propto \frac{1}{\prod_{k=1}^M |F_{b_k}|^{1/2}} \exp \left\{ -\frac{1}{2} \sum_{k=1}^M (w_{b_k} - B_{b_k} w_{N(b_k)})^T F_{b_k}^{-1} (w_{b_k} - B_{b_k} w_{N(b_k)}) \right\}. \end{aligned}$$

Let $w_{b_k} - B_{b_k} w_{N(b_k)} = B_{b_k}^* w_S$, and j be the j -th observation of block b_k , then $\forall k = 1, \dots, M$, $i = 1, \dots, n$ and $j = 1, \dots, n_{b_k}$:

$$B_{b_k}^*(j, i) = \begin{cases} 1 & \text{if } s_i \in s_{b_k} \\ B_{b_k}[j, l] & \text{if } s_i \in s_{b_k}; s_i = s_{N(b_k)}[l]; l = 1, \dots, N_{b_k} \\ 0 & \text{otherwise,} \end{cases}$$

and

$$B_{b_k}^* = \begin{bmatrix} B_{b_k}^*(1) \\ \vdots \\ B_{b_k}^*(j) \\ \vdots \\ B_{b_k}^*(n_{b_k}) \end{bmatrix}_{n_{b_k} \times n}.$$

From these definitions, $B_{b_k}^*$ is a matrix with i -th column full of zeros if $s_i \notin s_{b_k}$ or $s_i \notin N(s_{b_k})$. Since the data were reordered by blocks and the neighbor blocks are from the past, $B_{b_k}^*$ has the next form:

$$B_{b_k}^* = [R_k \quad \underline{A_k} \quad 0 \quad \dots \quad 0],$$

where A_k is a $n_{b_k} \times n_{b_k}$ matrix and R_k is a $n_{b_k} \times \sum_{r=1}^{k-1} n_{b_r}$ matrix with at least one column with none null-element if $nb \neq 0$.

Then,

$$\begin{aligned} \tilde{p}(w) &\propto \frac{1}{\prod_{k=1}^M |F_{b_k}|^{1/2}} \exp \left\{ -\frac{1}{2} \sum_{k=1}^M (B_{b_k}^* w_S)^T F_{b_k}^{-1} (B_{b_k}^* w_S) \right\} \\ &\propto \frac{1}{\prod_{k=1}^M |F_{b_k}|^{1/2}} \exp \left\{ -\frac{1}{2} \sum_{k=1}^M w_S^T (B_{b_k}^*)^T F_{b_k}^{-1} (B_{b_k}^* w_S) \right\} \\ &\propto \frac{1}{\prod_{k=1}^M |F_{b_k}|^{1/2}} \exp \left\{ -\frac{1}{2} \sum_{k=1}^M w_S^T ((B_{b_k}^*)^T F_{b_k}^{-1} B_{b_k}^*) w_S \right\} \\ &\propto \frac{1}{\prod_{k=1}^M |F_{b_k}|^{1/2}} \exp \left\{ -\frac{1}{2} w_S^T \left(\sum_{k=1}^M (B_{b_k}^*)^T F_{b_k}^{-1} B_{b_k}^* \right) w_S \right\}. \end{aligned}$$

Let $\sum_{k=1}^M (B_{b_k}^*)^T F_{b_k}^{-1} B_{b_k}^* = (B_s^*)^T F_s^{-1} B_s^*$, where $B_s = [B_{b_1}^* \quad \dots \quad \dots \quad B_{b_M}^*]$ and $F_s^{-1} = \text{diag}(F_{b_k}^{-1})$. F_s^{-1} is a block diagonal matrix and (iii) is proved. And given that $B_{b_k}^*$ is a matrix with i -th column full of zeros for $i > \sum_{r=1}^k n_{b_r}$, then B_s is a block matrix and lower triangular, and (ii) is proved.

Finally, $\tilde{p}(w) \propto \frac{1}{\prod_{k=1}^M |F_{b_k}|^{1/2}} \exp \left\{ -\frac{1}{2} w_S^T (B_s^T F_s^{-1} B_s) w_S \right\}$ and $\tilde{C}_s^{-1} = B_s^T F_s^{-1} B_s$.

\tilde{C}_s is positive definite

From properties of the Normal distribution, the covariance of the conditional distribution of $w_{b_k} | w_{N(b_k)}$ is also p.d. (by Schur complement conditions), then $F_{b_i} = C_{b_i} - C_{b_i, N(b_i)} C_{N(b_i)}^{-1} C_{N(b_i), b_i}$,

is p.d. Moreover, $F_s = \text{diag}(F_{b_i})$ and a block diagonal matrix is p.d. if and only if each diagonal block is positive definite, so given that F_{b_i} is p.d. and F_s is block diagonal with blocks F_{b_i} p.d then F_s is p.d. By Corollary A1, F_s is p.d. then F_s^{-1} is p.d. By Theorem A1, B_s has full column rank if and only if $R_s = B_s^T F_s B_s$ is invertible. By Theorem A2, the inverse of R_s exists iff $\det(R_s) \neq 0$. Using the well-known matrix theorems (Henderson and Searle, 1981), we can prove the following: $\det(R_s) = \det(B_s^T F_s B_s) = \det(B_s^T) \det(F_s) \neq 0$ if $\det(B_s^T) = \det(B_s) \neq 0$. Given that B_s is a lower triangular matrix, by Theorem A3, $\det(B_s) = \prod_{k=1}^n (b_{kk})$. Using, $b_{kk} = 1, \forall k$, then $\det(B_s) \neq 0$. So, the R_s is invertible and B_s has full column rank. By Proposition A1, given that B_s has full column rank, and F_s^{-1} is p.d. then $\tilde{C}_s^{-1} = B_s^T F_s^{-1} B_s$ is p.d. And by corollary A1, \tilde{C}_s^{-1} is p.d. then \tilde{C}_s is p.d. and (iv) is proved.

Since $\tilde{p}(w_S) \propto \frac{1}{\prod_{k=1}^M |F_{b_k}|^{1/2}} \exp \left\{ -\frac{1}{2} w_S^T (\tilde{C}_s^{-1}) w_S \right\}$, $\tilde{C}_s^{-1} = B_s^T F_s^{-1} B_s$, and \tilde{C}_s is p.d., then $\tilde{p}(w_S)$ is a pdf of a multivariate normal distribution and (i) is proved.

If $n_{bk} \ll n$ then $i > \sum_{r=1}^k n_{br}$ and $B_{b_k}^*$ will be more sparse. Also, if n_k is small, the block diagonal matrix F_s^{-1} will be more sparse. As result, $\tilde{C}_s^{-1} = B_s^T F_s^{-1} B_s$, will still be sparse. \square

Proof of Lemma 1. We need to prove that the finite dimensional distributions in Equation (4) are consistent with a stochastic process. The Kolmogorov consistency conditions are checked as follows:

Symmetry under permutation: Let π_1, \dots, π_n be any permutation of $1, \dots, n$, note that S is fixed, then it is clear that $\tilde{p}(w(v_1), \dots, w(v_n)) = \tilde{p}(w(v_{\pi_1}), \dots, w(v_{\pi_n}))$ if and only if the same holds for the distribution of $u_i | N(u_i)$. Since $w_U | w_S$ follows a l-multivariate normal distribution, then the symmetry condition is satisfied by $p(w_U | w_S)$, and it holds that the next condition $\tilde{p}(w(u_1), \dots, w(u_l) | w_S) = \tilde{p}(w(u_{\pi_1}), \dots, w(u_{\pi_l}) | w_S)$ is necessary and sufficient to prove the symmetry condition of $\tilde{p}(w_V)$. To prove this we define the next pdfs,

$$\begin{aligned} \tilde{p}(w(u_1), \dots, w(u_l) | w_S) &= |2\pi F_U|^{-1/2} \exp \left\{ -\frac{1}{2} (w_U - B_U w_S)^T F_U^{-1} (w_U - B_U w_S) \right\} \\ &= |2\pi F_U|^{-1/2} \exp \{ Q(w_U) \}, \end{aligned}$$

and

$$\begin{aligned} \tilde{p}(w(u_{\pi_1}), \dots, w(u_{\pi_l}) | w_S) &= |2\pi \Sigma'|^{-1/2} \exp \left\{ -\frac{1}{2} (w_{U\pi} - m')^T \Sigma'^{-1} (w_{U\pi} - m') \right\} \\ &= |2\pi \Sigma'|^{-1/2} \exp \{ Q(w_{U\pi}) \}. \end{aligned}$$

We also define a permutation matrix P such that $(\pi_1, \dots, \pi_l)^T = P(1, \dots, l)^T$. Then $Pw_U = P(w(u_1), \dots, w(u_l))^T = (w(u_{\pi_1}), \dots, w(u_{\pi_l}))^T = w_{U\pi}$. And the mean and covariance matrix of $w_{U\pi} | w_S$ are $m' = PB_U w_S$ and $\Sigma' = PF_U P'$. Since $P^{-1} = P^T$ it follows that $|P| = \pm 1$ which implies that $|\Sigma'| = |F_U|$. Using this we have,

$$\begin{aligned} Q(w_{U\pi}) &= (Pw_U - m')^T \Sigma'^{-1} (Pw_U - m') = (Pw_U - PB_U w_S)^T (PF_U P')^{-1} (Pw_U - PB_U w_S) = \\ &= (w_U - B_U w_S)^T P^T (P^T F_U^{-1} P^T) P (w_U - B_U w_S) = (w_U - B_U w_S)^T P^T \Sigma'^{-1} P (w_U - B_U w_S) = \end{aligned}$$

$$(w_U - B_U w_S)^T F_U^{-1} (w_U - B_U w_S) = Q(w_U).$$

Since both $|F_U|$ and $Q(w_U)$ are invariant under permutations, $\tilde{p}(w(u_1), \dots, w(u_l)|w_S) = \tilde{p}(w(u_{\pi_1}), \dots, w(u_{\pi_l})|w_S)$ and hence the symmetry condition is satisfied.

Dimensional consistency: We also assume that S is fixed, so, this proof does not differ from the one found in (Datta et al., 2016) although $\tilde{p}(w_S)$ has a different definition.

Let $V_1 = V \cup \{v_0\}$ then $V_1 = S' \cup \{v_0\} \cup U$. We need to verify $\tilde{p}(w_V) = \int \tilde{p}(w_{V_1}) d(w(v_0))$. So, we have two cases:

Case 1: If $v_0 \in S$. By definition $\tilde{p}(w_{V_1}) = \int \tilde{p}(w_{V_1|S}|w_S) \tilde{p}(w_S) \prod_{si \in S|V_1} d(w_{s_i})$, then

$$\int \tilde{p}(w_{V_1}) d(w(v_0)) = \int \tilde{p}(w_{V_1|S}|w_S) \tilde{p}(w_S) \prod_{si \in S|V_1} d(w_{s_i}) d(w(v_0)).$$

If $v_0 \in S$, and $V = S' \cup U$ then $v_0 \in (S')^c$, and $\prod_{si \in S|V_1} d(w_{s_i}) d(w(v_0)) = \prod_{si \in (S')^c} d(w_{s_i})$, and

$$\int \tilde{p}(w_{V_1}) d(w(v_0)) = \int \tilde{p}(w_{V_1|S}|w_S) \tilde{p}(w_S) \prod_{si \in (S')^c} d(w_{s_i}).$$

Also, $V_1|S = U$ since $v_0 \in S$, then

$$\int \tilde{p}(w_{V_1}) d(w(v_0)) = \int \tilde{p}(w_U|w_S) \tilde{p}(w_S) \prod_{si \in (S')^c} d(w_{s_i}) = \tilde{p}(w_V).$$

Case 2: If $v_0 \notin S$, then $V_1|S = U \cup \{v_0\}$, $\tilde{p}(w_{V_1|S}|w_S) = \tilde{p}(w_U|w_S) \tilde{p}(w(v_0)|w_S)$ and $S|V_1 = (S')^c$. Now,

$$\begin{aligned} \tilde{p}(w_{V_1}) &= \int \tilde{p}(w_{V_1|S}|w_S) \tilde{p}(w_S) \prod_{si \in S|V_1} d(w_{s_i}) \\ &= \int \tilde{p}(w_U|w_S) \tilde{p}(w(v_0)|w_S) \tilde{p}(w_S) \prod_{si \in (S')^c} d(w_{s_i}). \end{aligned}$$

Hence,

$$\begin{aligned} \int \tilde{p}(w_{V_1}) d(w(v_0)) &= \int \tilde{p}(w_U|w_S) \tilde{p}(w(v_0)|w_S) \tilde{p}(w_S) \prod_{si \in (S')^c} d(w_{s_i}) d(w(v_0)) \\ &= \int \tilde{p}(w_S) \tilde{p}(w_U|w_S) [\tilde{p}(w(v_0)|w_S) d(w(v_0))] \prod_{si \in (S')^c} d(w_{s_i}), \end{aligned}$$

where $\int \tilde{p}(w(v_0)|w_S) d(w(v_0)) = 1$, since $w(v_0)$ does not appear in any other term. Finally,

$$\int \tilde{p}(w_{V_1}) d(w(v_0)) = \int \tilde{p}(w_S) \tilde{p}(w_U|w_S) \prod_{si \in (S')^c} d(w_{s_i}) = \tilde{p}(w_V).$$

□

Proof of Theorem 1. To verify that $\tilde{p}(w_V)$ is the pdf of finite dimensional distribution of a Gaussian process, only rests to prove that $\tilde{p}(w_V)$ is the pdf of a multivariate normal distribution. Since $w_U|w_S$ follows a l-multivariate normal distribution and w_S follows a n-multivariate normal distribution, the product of these densities is also a multivariate normal distribution.

Let $\tilde{C}_{m,n}$ is the covariance matrix of \tilde{C}_S . The cross-covariance is computed for the next possible cases:

Case 1: If $v_1 \in S$ and $v_2 \in S$, that is, $v_1 = s_i$ and $v_2 = s_j$, then $\text{cov}(w(v_1), w(v_2)|\theta) = \tilde{C}_{s_i, s_j}$.

Case 2: If $v_1 \in U$ and $v_2 \in S$, we may suppose also that $v_2 \in b_l$. Using the law of total covariance,

$$\text{cov}(w(v_1), w(v_2)|\theta) = E(\text{cov}(w(v_1), w(v_2)|w_S)|\theta) + \text{cov}(E(w(v_1)|w_S), E(w(v_2)|w_S)|\theta).$$

From our definition $w(v_1)|w_S \perp w(b_l)|w_S$ and $v_2 \in b_l$, then we have that $w(v_1)|w_S \perp w(v_2)|w_S$ and $\text{cov}(w(v_1)|w_S, w(v_2)|w_S) = 0$. Further, $E(w(v_1)|w_S) = B_{v_1}w_{N(v_1)}$ and using the next property, $E(g(X)|X) = g(X)$, $E(w(v_2)|w_S) = w(v_2)$. It follows that,

$$\text{cov}(w(v_1), w(v_2)|\theta) = E(0|\theta) + \text{cov}(B_{v_1}w_{N(v_1)}, w(v_2)|\theta) = B_{v_1}\tilde{C}_{N(v_1), w(v_2)} = B_{v_1}\tilde{C}_{N(v_1), w(s_j)}.$$

Case 3: If $v_1 \in U$ and $v_2 \in U$. This part of the proof is the same for the NNGP, found in (Datta et al., 2016). We have $E(w(v_1)|w_S) = B_{v_1}w_{N(v_1)}$ and $E(w(v_2)|w_S) = B_{v_2}w_{N(v_2)}$. Then,

$$\begin{aligned} \text{cov}(E(w(v_1)|w_S), E(w(v_2)|w_S)|\theta) &= \text{cov}(B_{v_1}w_{N(v_1)}, B_{v_2}w_{N(v_2)}) \\ &= B_{v_1}\text{cov}(w_{N(v_1)}, w_{N(v_2)})B_{v_2}^T. \end{aligned}$$

Observe that if $v_1 \neq v_2$, then $w(v_1)|w_S \perp w(v_2)|w_S$ and $\text{cov}(w(v_1), w(v_2)|w_S) = 0$. Conversely, if $v_1 = v_2$ now $\text{cov}(w(v_1), w(v_2)|w_S) = \text{var}(w(v_1)|w_S) = F_{v_1}$. Then, $\text{cov}(w(v_1), w(v_2)|w_S) = \delta(v_1 = v_2)F_{v_1}$, and $E(\delta(v_1 = v_2)F_{v_1}|\theta) = \delta(v_1 = v_2)F_{v_1}$. Hence,

$$\text{cov}(w(v_1), w(v_2)|\theta) = \delta(v_1 = v_2)F_{v_1} + B_{v_1}\tilde{C}_{N(v_1), N(v_2)}B_{v_2}^T.$$

□

B: Supplementary Material

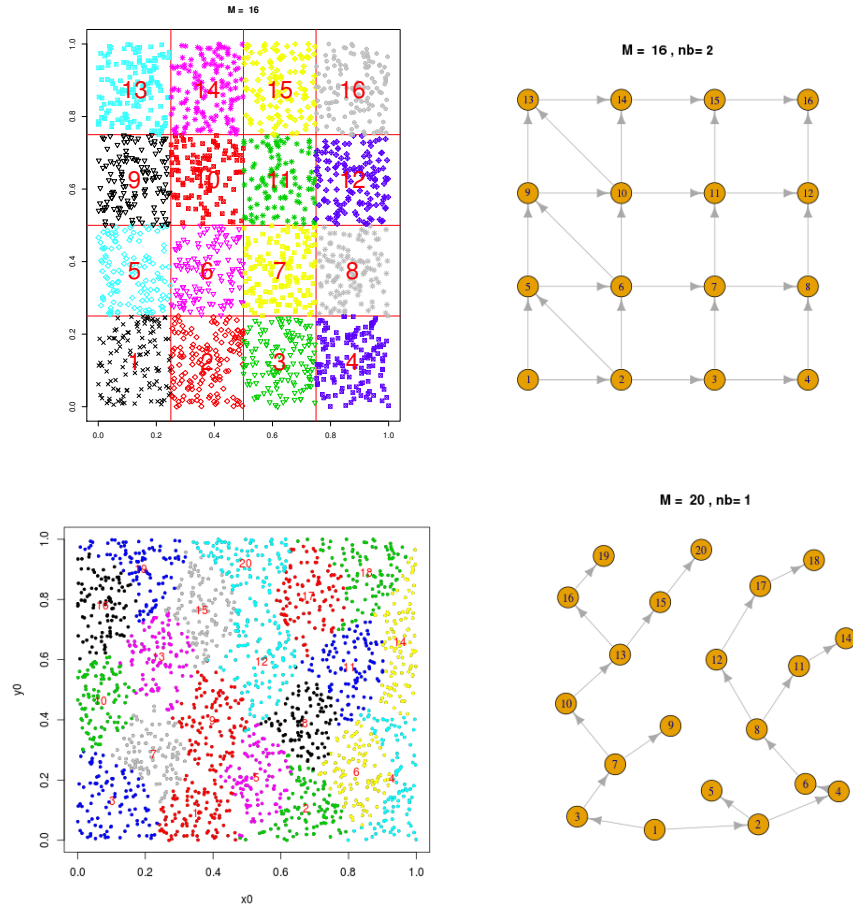


Figure S1: First row: Regular block. Second row: Irregular block. Left: Block design. Right: DAG of blocks.

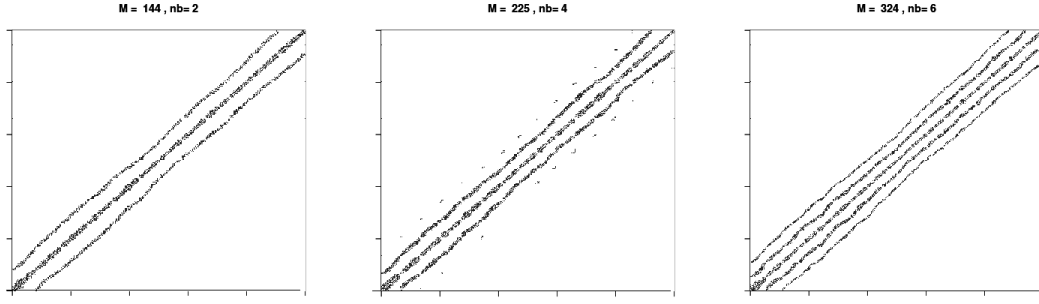


Figure S2: Sparse pattern of precision matrices \tilde{C}_S^{-1} of block-NNGP, with different number of blocks (M) and different number of neighbor blocks (nb). Only the nonzero terms are shown and those are indicated by a dot.